京都大学防災研究所年報 第 56 号 B 平成 25 年 6 月
Annuals of Disas. Prev. Res. Inst., Kyoto Univ., No. 56 B, 2013

Assessment of High-resolution Ensemble NWP Rainfall for Flood Forecast of Relative Large River Basin in Japan

Wansik YU [(1)], Eiichi NAKAKITA[(2)] and Kosei YAMAGUCHI [(2)]

(1) Graduate School of Engineering, Kyoto University
(2) Disaster Prevention Research Institute, Kyoto University

Synopsis

In early September, 2011, Typhoon Talas caused local heavy rainfalls over the Kinki, Chugoku, Shikoku and Tokai regions in Japan. In these types of extreme events, it is essential to be able to provide as much advance warning as possible. This advance warning requires both quantitative precipitation forecasting (QPF) and quantitative flood forecasting (QFF). The operational meso-scale model of the JMA generally predicted the typhoon track well in the early period. However, the rainfall intensity was weaker than expected, and the movement was also faster when the lead time was longer. The latest ensemble NWP forecast with 30hr forecast time and 2km horizontal resolution has been generated by the Meteorological Research Institute (MRI) of the JMA. In this study, we assessed the latest ensemble NWP outputs with 30hr forecast time and 2km horizontal resolution from MRI whether they can produce suitable rainfall predictions or not during the Typhoon Talas event, and we also assessed the performance of ensemble flood forecasting for hydrological applications based on the latest ensemble NWP forecast with 30hr forecast time and 2km horizontal resolution. As a result, ensemble rainfall prediction produced more suitable results compared with a deterministic control run in terms of QPF. Ensemble flood forecasting driven by ensemble rainfall forecasts could also produce comparable results in comparisons of observed data, although the maximum peak discharge value was underestimated.

Keywords: Typhoon Talas, Ensemble NWP rainfall, Ensemble Flood Forecasting

1. Introduction

In early September, 2011, local heavy rainfalls due to season's 12th typhoon, "Talas" caused large flooding and enormous landslide disasters over the Kinki, Chugoku, Shikoku, and Tokai regions in Japan. It also caused unprecedented human damages, resulting in 78 dead and 16 missing persons. Talas moved very slowly and had a huge gale diameter throughout its life. The total amount of the precipitation exceeded 1,000mm in the Kii Peninsula.

One of the main challenges in these types of extreme events, it is principal to be able to provide as much advance warning as possible with extended lead time. This advance warning requires both quantitative precipitation forecasting (QPF) and quantitative flood forecasting (QFF). Traditionally, QPF can be obtained through the use of extrapolation of movement pattern of rainfall distribution from a sequence of radar image or through the use of solving numerically the equations of Numerical Weather Prediction (NWP) model. However, radar forecasting techniques using

extrapolation of movement pattern do not consider such as growth and decay of precipitation. On the other hand, NWP models use current weather conditions as input to atmospheric models to predict the evolution of weather systems. These models represent the atmosphere as a dynamic fluid and solve for its behavior through the use of mechanics and thermodynamics (Nakakita et al., 1996). However, the rainfall prediction using NWP models is difficult because the atmosphere is a nonlinear, chaotic system. A slight change in the initial and boundary layer conditions of a system could result in unpredictable results. In addition, unavoidable random errors in atmospheric model parameters make it difficult for NWP models to compute atmospheric properties accurately (Buizza et al., 1999). The Meso-Scale Model (MSM) of Japan Meteorological Agency (JMA) is now run operationally with a horizontal resolution of 5km. During the Typhoon Talas event, the MSM generally predicted the typhoon track well in the early period. However, the predicted rainfall intensity was weaker than the observed radar rainfall, and the movement was also faster, as the lead time was longer. As a result, the rainfall forecast pattern moved to the north-eastern part of the Kii peninsula quickly. One of the methods to overcome the forecast failure of deterministic predictions is to use ensemble outputs of NWP models. Ensemble NWP rainfall has been generated since the early 1990s. It is believed that ensemble prediction systems exhibit greater forecast skill than a single NWP model (Buizza et al., 1999; Demeritt et al., 2007). Another method for an improvement in accuracy can be achieved by increasing in the resolution of NWP models. In Japan, the JMA's operational one-week ensemble prediction has been developed to support typhoon track forecast and to provide probabilistic information with a horizontal resolution of 60km and 51 Ensemble members. However, there is a limitation to use one-week ensemble prediction in respect of hydrological applications because one-week ensemble prediction has a coarse spatial resolution. With consideration for high-resolution and ensemble forecasts, the latest ensemble NWP forecast with 30hr forecast time and 2km horizontal resolution has been generated by the Meteorological Research Institute (MRI) of the JMA, and is still in research for an improvement in terms of the forecast accuracy. This ensemble NWP forecast is not yet operational, and it is expected that this ensemble NWP prediction can improve the forecast skill more than operational deterministic rainfall forecasts.

In the context of flood management, it is important to integrate NWP model output and flood forecasts. It is possible to incorporate NWP model outputs directly into flood forecasting systems to obtain an extended lead time (Xuan et al., 2009). However, direct application of deterministic NWP model output can propagate uncertainties into the hydrologic domain. For these reasons, the development of ensemble hydrological applications started in the late 1990s and is a field of ongoing research (De Roo et al., 2003; Gouweleeuw et al., 2005). Ensemble flood forecasting provides additional information to the deterministic flood forecast in the short forecast range, and provides a signal in terms of pre-warning and exceedance probabilities for threshold values (e.g. critical discharge, levels causing inundation, and so on).

In this study, we aim to overcome an insufficiency of the deterministic flood forecast using ensemble outputs with 30hr forecast time and 2km high-resolution. Therefore, we assess the latest ensemble NWP outputs with 30hr forecast time and 2km horizontal resolution from MRI whether they can produce suitable rainfall predictions or not during the Typhoon Talas event, and we also assess the performance of ensemble flood forecasting for hydrological applications based on the latest ensemble NWP forecast with 30hr forecast time and 2km horizontal resolution.

2. METHODOLOGY

2.1 Short-range ensemble rainfall forecast

We used two ensemble systems with 10km and 2km horizontal resolution. The latest forecast model was developed and implemented by MRI of JMA for rainfall forecast using nonhydrostatic model (Saito et al., 2006). Whereas the 10km resolution forecast adopted the cloud microphysical process and Kain-Fritsch convective scheme, the 2km resolution forecast did not have to use a convective

scheme because of its cloud resolving resolutions. The ensemble system consists of 10 perturbed and one unperturbed (or control run). One forecast, the "control run," is forecast with a non-perturbed analysis and is similar to the MSM of JMA from the viewpoints of initial and lateral boundary conditions. The 10 perturbed forecasts of ensemble system result from a perturbation technique based on a mathematical method called the local ensemble transform Kalman filter (LETKF) method (Miyoshi, 2010).

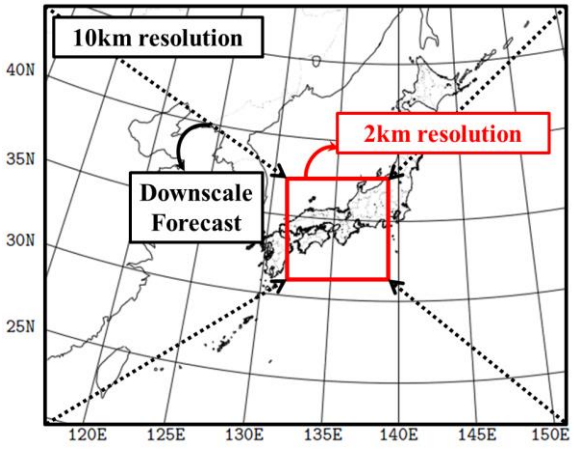

Fig. 1 Forecast domains of 10km and 2km horizontal resolution

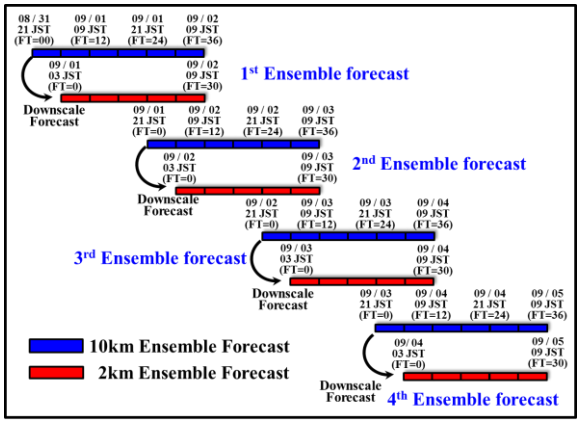

Fig. 2 A schematic of four sets of forecast runs (blue and red boxes denote the 10km and 2km horizontal resolutions, respectively.)

The domain of the two ensemble systems with 10km and 2km horizontal resolution are illustrated in Fig. 1. The 10km and the 2km resolutions had a domain of 361×289 grid points and 350×350 grid, respectively. At first, a meso ensemble prediction with a horizontal resolution of 10km was performed up to 36hr forecast time at 9pm JST, and its downscale prediction with a horizontal resolution of 2km was performed up to 30hr forecast at 3am JST. Initial conditions of the 2km ensemble forecast were given by the 6hr forecast time of the 10km ensemble forecast results. This process is continued during the Typhoon Talas event. Therefore, we constructed the 4 sets of ensemble prediction outputs with 10km and 2km horizontal resolution (Fig. 2), and we introduce the results of ensemble prediction with 2km horizontal resolution due to the viewpoints of high-resolution and better predictability of weather phenomena in this study. Fig 4 shows the ensemble NWP rainfall forecast of 2km horizontal resolution during Typhoon Talas (2011/09/02/15:00 JST).

2.2 Distributed grid-based hydrologic model

We used the grid-based one-dimensional kinematic wave method for subsurface and surface flow simulation, which was enhanced by Tachikawa et al. In this model, the drainage network is represented by sets of hillslope and channel elements from the digital elevation model. Each element is represented by a rectangle formed by two adjacent nodes of grid cells. Fig. 3 is a schematic of spatial flow movement in this model.

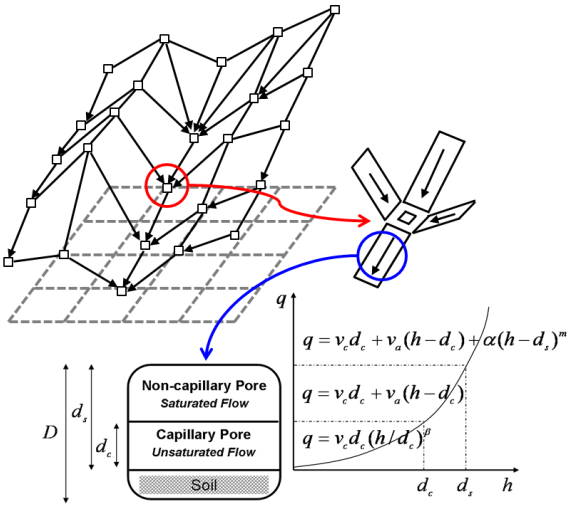

Fig. 3 Spatial flow movement: the arrows indicate element models for calculating hydrological variables, such as water flux and stage–discharge relationship of flow process in the hillslope elements.

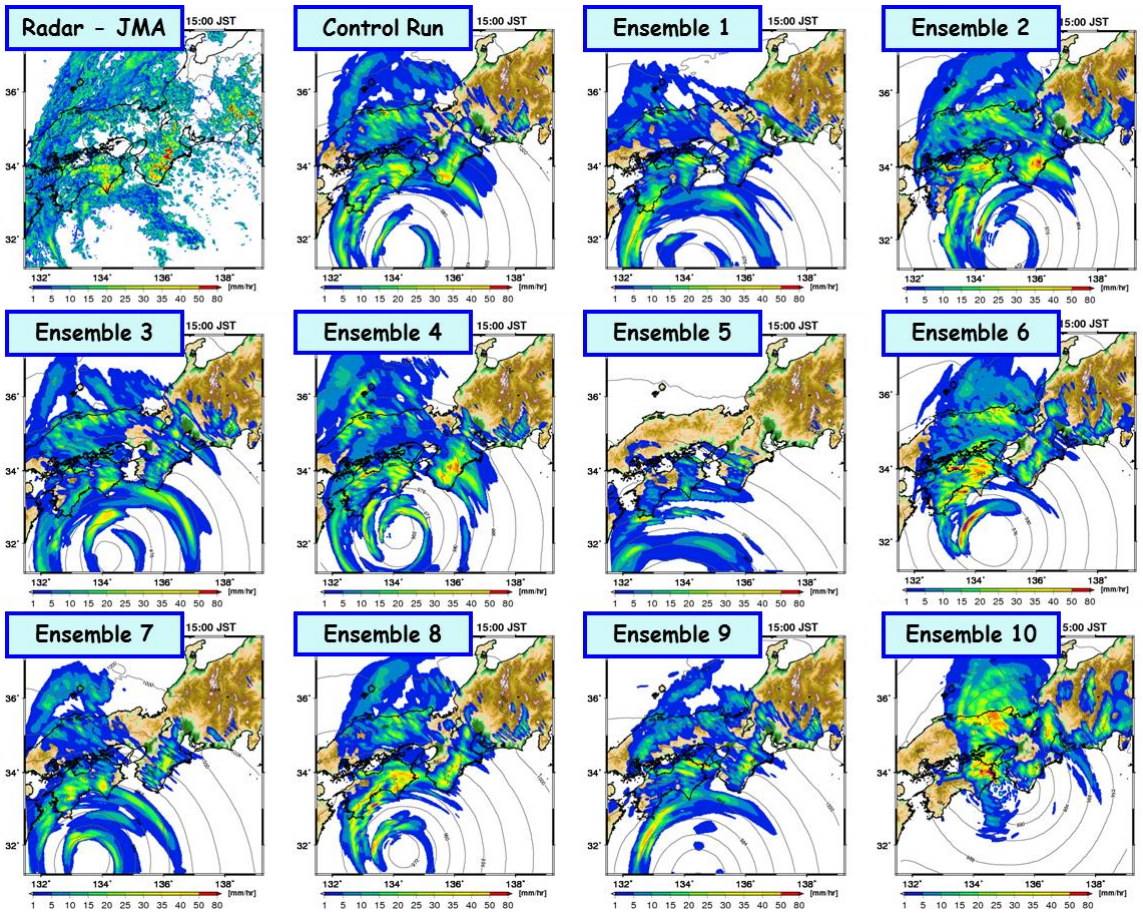

Fig. 4 Ensemble NWP rainfall forecast of 2km horizontal resolution (2011/09/02/15:00JST)

The rainfall over all hillslope elements flows one-dimensionally into the river nodes and then routes to the catchment outlet. The rainfall-runoff transformation is based on the assumption that each hillslope element is covered with a permeable soil layer. This soil layer consists of a capillary layer and a non-capillary layer. In these conceptual soil layers, slow and quick flow are simulated as unsaturated and saturated flow, respectively, and surface flow occurs if water depth, h (m) exceeds soil water capacity.

$$q = \begin{cases} v_c d_c (h/d_c)^{\beta}, & 0 \le h \le d_c \\ v_c d_c + v_a (h - d_c), & d_c \le h \le d_s \\ v_c d_c + v_a (h - d_c) + \alpha (h - d_s)^m, & d_s \le h \end{cases} \quad (1)$$

$$\frac{\partial h}{\partial t} + \frac{\partial q}{\partial x} = r(x,t) \quad (2)$$

The discharge per unit width q [m^2/s] is calculated by Eq. (1), combined with the continuity equation, Eq. (2), where t is the time (s), x is space (m), r(t) is the rainfall intensity (mm/h), $v_c = k_c i$ (m/s), $v_a = k_a i$ (m/s), $k_c = k_a / \beta$ (m/s), $\alpha = \sqrt{i}/n$ ($m^{1/3}$/s), m=5/3, i is the slope gradient, k_c (m/s) is the hydraulic conductivity of the capillary soil layer, k_a (m/s) is the hydraulic conductivity of the non-capillary soil layer, n ($m^{1/3}$/s) is the roughness coefficient, and d_c and d_s are soil depth in the capillary and non-capillary pore, respectively. Rainfall is directly added to subsurface or surface flow on grid cells according to the water depth of each cell corresponding to parts of the rainfall input field. This model does not consider vertical flow due to infiltration, but represents lagged subsurface flow with calibrated hydraulic conductivities and soil layer thicknesses.

3. Results and discussion

3.1 Study area

Typhoon Talas caused enormous flooding and landslide disasters in the Shingu River Basin, and many roads were damaged as well as electricity, communication lines and water supply.

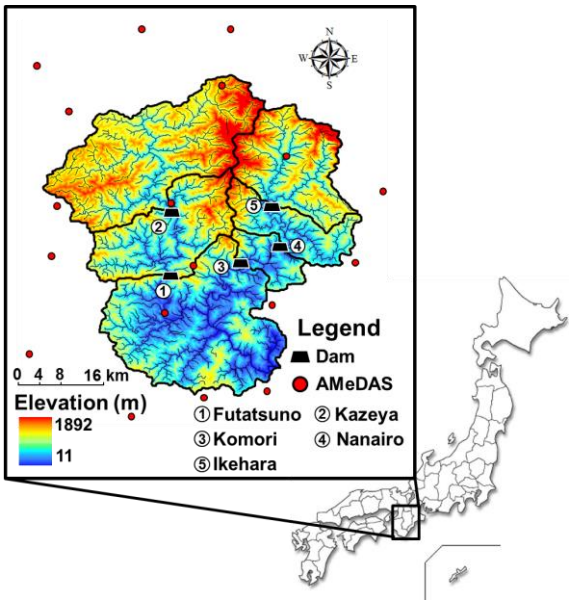

Fig. 5 Study area (Kumano River Basin) within Kii peninsula in Japan.

Therefore, in this study, we selected the Shingu River Basin as the study area to assess the flood forecast applicability utilizing the ensemble NWP rainfall. Shingu River Basin is located in the Kii peninsula of the Kinki region, Japan and covers an area of 2,360 km^2 (Fig. 5). The topography of the basin is characterized by a mountainous upstream in the north and a flatter plain in the south. The elevation in the basin ranges from 11 to 1892 m, with an average of about 644 m. The five dams Futatsuno, Kazeya, Komori, Nanairo and Ikehara are located upstream.

3.2 Ensemble NWP rainfall

For the purpose of temporal verification of QPF with ensemble NWP rainfall during the Talas event, we compared the areal rainfall intensity between the Automated Meteorological Data Acquisition System (AMeDAS) and ensemble prediction over the Shingu River Basin in the form of box plots. For comparison, the observed rainfall of AMeDAS (18 stations, 10min step) is interpolated using the Thiessen polygon spatial distribution method. In the 1st and 2nd forecast period of Fig. 6(a), the control run and ensemble forecast produced a suitable areal rainfall compared with the AMeDAS rainfall, but as shown in the 3rd forecast result, on which focused in this study, the control run forecast was well not matched and did not produce the rainfall intensity because the spatial pattern of raincells moved to the north-eastern part of Kii peninsula quickly by that the MSM failed to correctly forecast, as mentioned in the introduction section. On the other hand, the upper range of the ensemble forecast was able to produce considerable rainfall intensity, and the amounts of maximum rainfall intensity are also similar to AMeDAS rainfall. In 4th forecast period, the reason why rainfall intensities are overestimated can be explained by the fact that the last spatial rainfall pattern of the 3rd forecast moved to the north-eastern part of the Kii peninsula; however, it

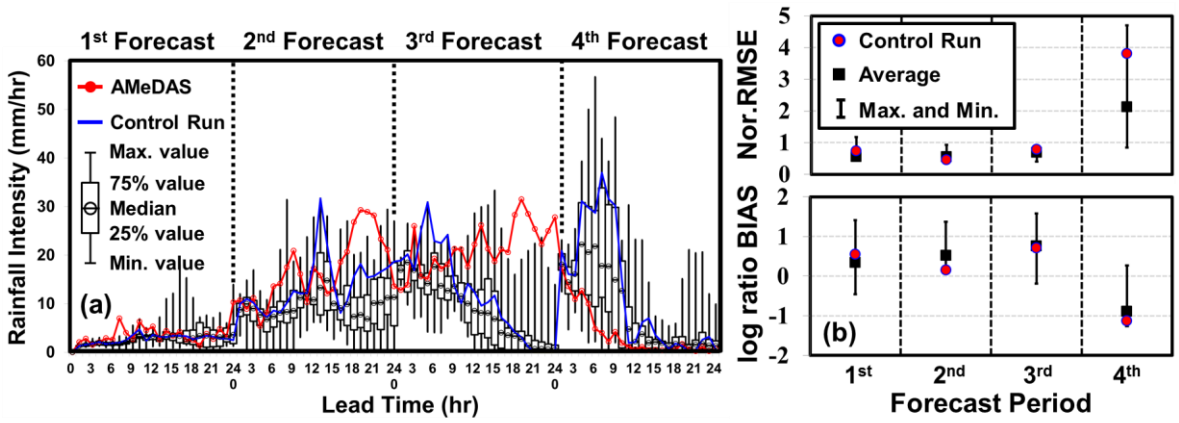

Fig. 6 (a) Ensemble areal rainfall forecast over the Shingu River Basin in the form of box plots plotted from 0 to 24hr forecast time, excluding overlapped forecast time (from 25 to 30hr) for the overall comparison for the Typhoon Talas. (b) Verification results of areal rainfall with normalized RMSE and log ratio bias for Typhoon Talas. Red circles and black squares mean the indexes of the control run and the mean value of ensemble forecast, respectively. The lower and upper bounds of the black lines correspond to the minimum and maximum values, respectively.

started the forecast again from the Kii peninsula in the 4th forecast. For this reason, rainfall intensities were very high in the 4th forecast period compared with AMeDAS.

To evaluate the accuracy of the control run and ensemble forecast in terms of areal rainfall intensity, we calculated two error indexes (Fig. 6(b)). The first is the normalized root mean square error (RMSE, Eq. (3)), which is normalized by the mean value of the observations during the each forecast period (30hr). The second is the log ratio bias (Eq. (3)), which a relative error and provides information about the total amount of rainfall. A log ratio bias value of zero indicates a perfect forecast; positive and negative values indicate underestimated and overestimated forecasts, respectively.

$$Nor.RMSE = \frac{\sqrt{\frac{1}{N}\sum_{t=1}^{N}\left(X_t^{obs} - X_t^{pred}\right)^2}}{\overline{X^{obs}}} \quad (3)$$

$$\log\ ratio\ bias = \log\frac{\sum_{t=1}^{N} X_t^{obs}}{\sum_{t=1}^{N} X_t^{pred}} \quad (4)$$

In the index of normalized RMSE, the control run and ensemble mean have similar values from 1st to 3rd forecast period, but the best index of the ensemble forecast could provide good value as compared with the deterministic control run. In the 4th forecast period, as mentioned above, the index of the control run and ensemble spread is relatively large, but the best index of the ensemble is estimated at 0.84 (the control run is 3.81). In the index of the log ratio bias, the best index of ensemble spread was close to zero value (perfect forecast), whereas the control run forecast was underestimated for the 1st, 2nd, and 3rd forecasts, and overestimated for the 4th forecast period.

3.3 Ensemble flood forecast

We considered five dams located in the Shingu River Basin: Kazeya, Futatsuno, Ikehara, Nanairo and Komori dams for an assessment of the ensemble flood forecast driven by ensemble NWP rainfall in this study. Kazeya dam is in the upstream of the Futatsuno dam basin, and Ikehara and Nanairo dams are in the upstream of the Komori dam basin, respectively. The outflow record from each upstream dam was considered input data in a distributed hydrologic model. First, we conducted the parameter optimization of the hydrologic model

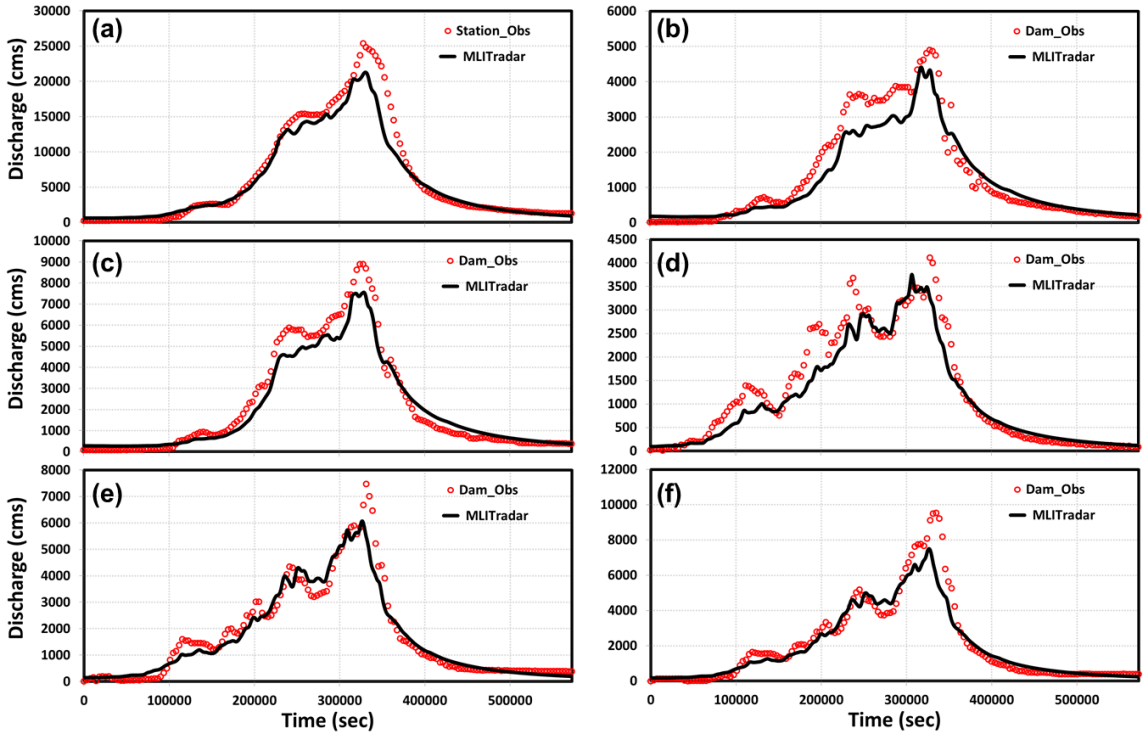

Fig. 7 Multi-gauge model calibration results; (a) Ouga station, (b) Kazeya dam, (c) Futatsuno dam, (d) Ikehara dam, (e) Nanairo dam, (f) Komori dam

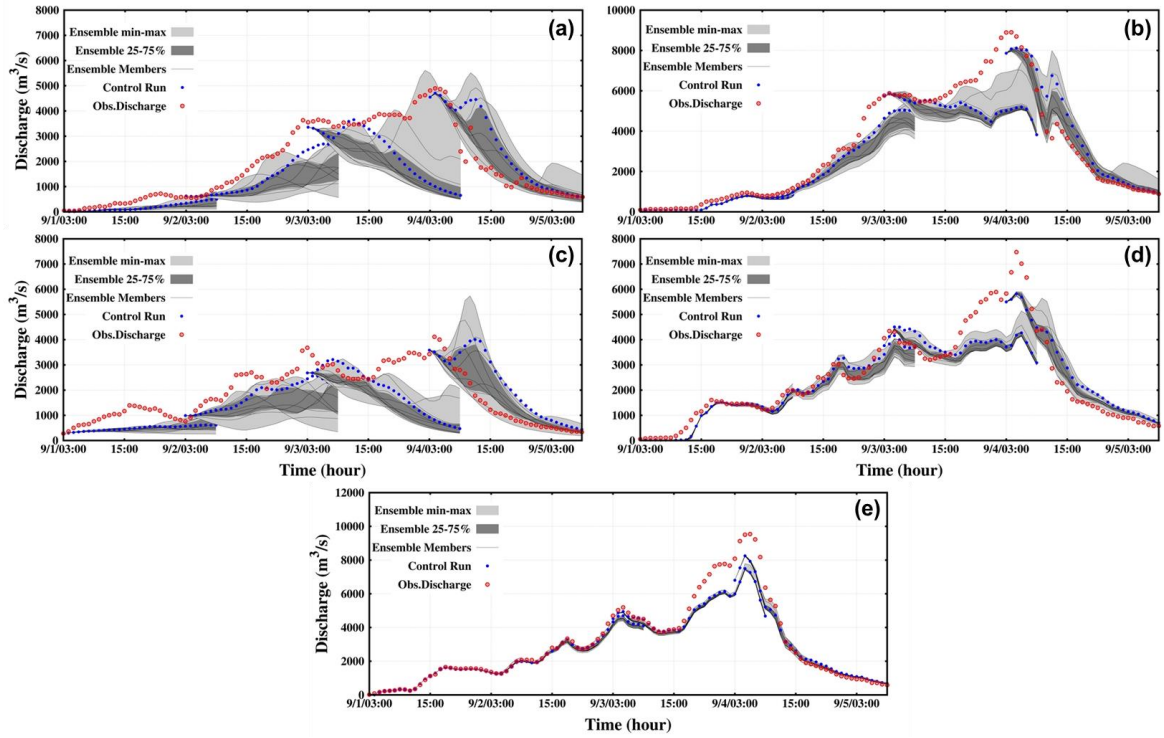

Fig. 8 30hr ensemble flood forecast from a distributed hydrologic model for Typhoon Talas; (a) Kazeya dam, (b) Futatsuno dam, (c) Ikehara dam, (d) Nanairo dam, (e) Komori dam

using MLIT composite radar data and Shuffled Complex Evolution (SCE) global optimization method. The SCE method is a general-purpose global optimization strategy designed to solve the various response surface problems encountered in calibrating a non-linear simulation model (Duan et al., 1994). In this study, there are upstream five dams and observed inflow data in the Shingu River Basin. Therefore we modified the SCE optimization method to minimize the objective function between observed inflows and simulated results at the same time for all of observation points (eq. (5)). Fig. 7 shows the results of multi-gauge model calibration using SCE optimization method minimizing the objective function of six observation points.

$$Minimize\ OF = \sum_{basin=1}^{n} RMSE_{Basin} \qquad (5)$$

Next, we used the simulated discharge from the observed radar rainfall as the initial condition for the ensemble flood forecast driven by the ensemble NWP rainfall. Fig. 8 shows the results of the 30hr ensemble flood forecast over the Kazeya, Futatsuno, Ikehara, Nanairo and Komori dams for Typhoon Talas. In the 3rd forecast period of peak discharge, on which we focused in this study, the control run forecast was typically lower than the observed discharge, caused by its shift from the correct spatial position. The majority of ensemble members were also lower than the observed discharge, but a few ensemble members exceeded the control run forecast, and were close to the observed discharge. In the 4th forecast period (falling limb), both the control run and ensemble forecast were overestimated because the over-estimation in rainfall forecast (4th forecast of Fig. 6(a)) triggered a runoff over-estimation.

To evaluate the accuracy of the control run and ensemble forecast in terms of discharge, we also used two error indexes, a normalized RMSE and a log ratio bias (Eq. (3) and (4)). Fig. 9 shows the results of normalized RMSE and log ratio bias for assessment of ensemble flood forecast. In the index of normalized RMSE, the ensemble flood forecast could provide good value as compared with the deterministic control run throughout all of dams, although the ensemble spread is relatively large. In the index of the log ratio bias, the ensemble spread was close to zero value, whereas the control run forecast was underestimated for the 1st, 2nd, and 3rd forecasts, and overestimated for the 4th forecast period. In these results, the ensemble flood

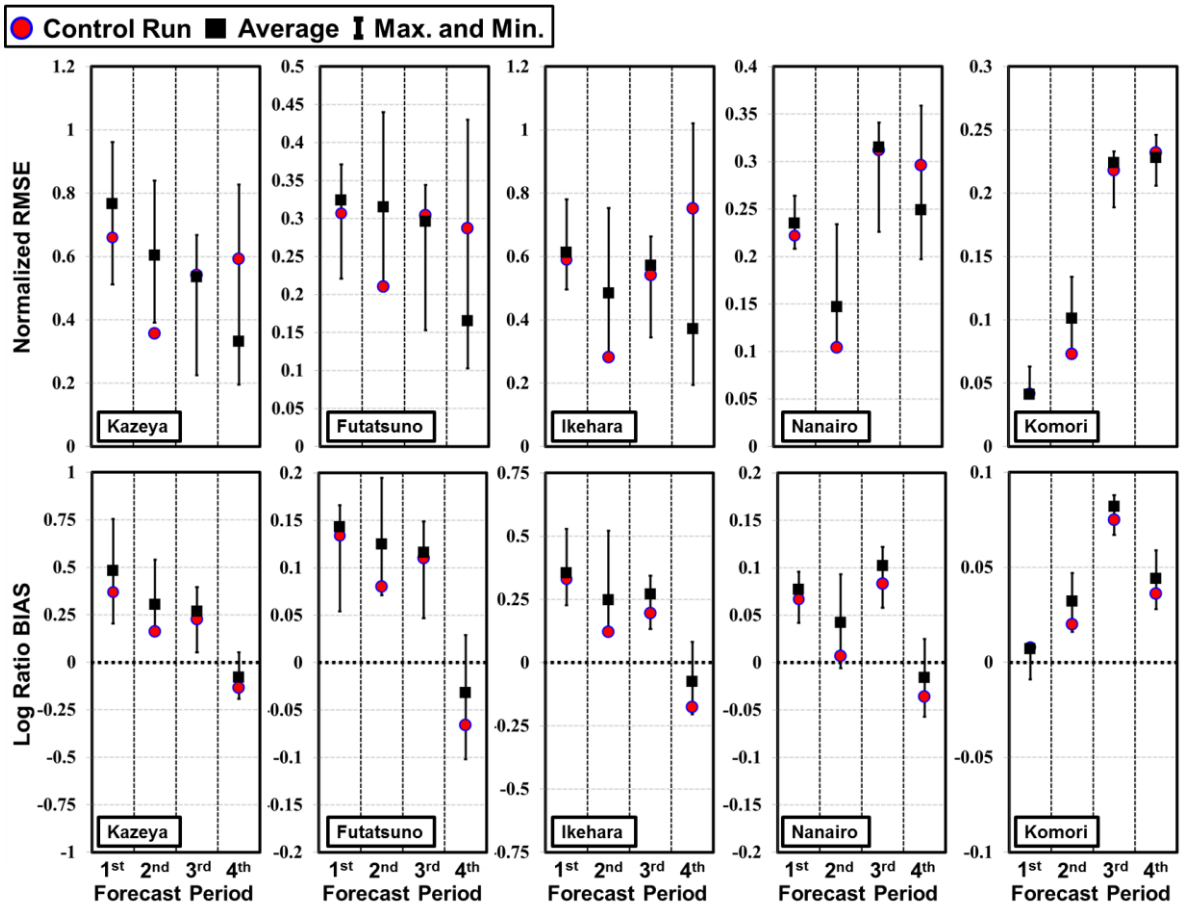

Fig. 9 Verification results of control run and ensemble runoff with normalized RMSE and log ratio bias for typhoon Talas

forecasts provided additional information that were not present in the deterministic forecast, and this additional information could be used for real-time flood forecast, dam inflow forecast, and dam release support. How this information should put into decision support, however, needs to be examined in more detail using a number of case studies to assess the performance of the probabilistic forecasts.

4. CONCLUSION

Flood forecast driven by ensemble-based NWP rainfall was carried out in this study to assess the hydrological applicability during the Typhoon Talas event. It can be concluded from the study that ensemble NWP rainfall produced better results as compared with deterministic control run in terms of QPF, and the study showed that the ensemble flood forecasts provide more suitable results and additional information that is not present in the deterministic forecast, although peak discharge value was underestimated. In further research, through a number of case studies, ensemble NWP rainfall data could be used in hydrological applications such as real-time flood forecasting and dam operation.

Acknowledgements

This study was partly supported by the sub-project of the field 3 on Next Generation Supercomputer Project, ‘Prediction of heavy rainfalls by a cloud-resolving NWP system’, and was based on data from J-POWER CO. Ltd. We are grateful for their support.

References

Buizza, R., Miller. M., and Palmer, T.N. (1999): Stochastic representation of model uncertainties in the ECMWF Ensemble Prediction System. Quart. J. Roy. Meteor. Soc., Vol.125, pp. 2887-2908.

Demeritt. D., Cloke. H., Pappenberger. F., Thielen.

J., Bartholmes. J. and Ramos. M.H. (2007): Ensemble predictions and perceptions of risk, uncertainty, and error in flood forecasting. Environ. Hazards, Vol.7, pp. 115-127.

De Roo, A., Gouweleeuw, B., Thielen, J., et al. (2003): Development of a European Flood Forecasting System, Intl. J. River Basin Management, Vol. 1, No. 1, pp. 49-59.

Duan, Q., Sorooshian, S. and Gupta, V.K. (1994): Optimal use of the SCE-UA global optimization method for calibrating watershed models, J. Hydrol., Vol.158, pp.265-284.

Gouweleeuw, B., Thielen, J., Franchello, G., De Roo, A. and Buizza, R. (2005): Flood forecasting using medium-range probabilistic weather prediction, Hydrol. Earth Syst. Sci., Vol.9, No.4, pp. 365-380.

Miyoshi, T. (2010): NHM-LETKF. Tech. Rep. MRI 62, pp. 159-163.

Nakakita. E., Ikebuchi. S., Nakamura. T., Kanmuri. M., Okuda. M., Yamaji. A. and Takasao. T. (1996): Short-term rainfall prediction methid using a volume scanning radar and grid point value data from numerical weather prediction. Journal of Geo. Research, Vol.101, No.D21, pp. 26,181-26,197.

Saito, K., Fujita T., Yamada Y., Ishida J., Kumagai Y., Aranami K., Ohmori S., Nagasawa R., Kumagai S., Muroi C., Katao T., Eito H., and Yamazaki Y. (2006): The operational JMA Nonhydrostatic Meso-scale Model. Mon. Wea. Rev., Vol.134, pp. 1266–1298.

Tachikawa, Y., Nagatani, G. and Takara, K. (2004): Development of stage-discharge relationship equation incorporating saturated–unsaturated flow mechanism. Annual Journal of Hydraulic Eng, JSCE, No.48, pp. 7-12 (in Japanese).

Xuan, Y., Cluckie, I. D. and Wang, Y. (2009): Uncertainty analysis of hydrological ensemble forecasts in a distributed model utilising short-range rainfall prediction. Hydrol. Earth Syst. Sci., Vol.13, pp.293-303.

(Received June 11, 2013)